Journal of
Medicinal Chemistry

Article

Identification of Reversible Small Molecule Inhibitors of Endothelial Lipase (EL) which Demonstrate HDL-C Increase In Vivo

George O. Tora, Soong-Hoon Kim, Zulan Pi, James A. Johnson, Ji Jiang, Monique S. Phillips, John L. Lloyd, Lynn Abell, Hao Lu, Gregory Locke, Leonard Adam, David Taylor, Xiaohong Yin, Kamelia Behnia, Lei Zhao, Richard Yang, Michael Basso, Christian Caporuscio, Alice ye Chen, Eddy Liu, Todd G. Kirchgessner, Joelle M. Onorato, Carol Ryan, Sarah C. Traeger, David A. Gordon, Ruth R. Wexler, and Heather J. Finlay

J. Med. Chem., **Just Accepted Manuscript** • DOI: 10.1021/acs.jmedchem.9b01831 • Publication Date (Web): 28 Jan 2020

Just Accepted

is published by the American Chemical Society. 1155 Sixteenth Street N.W., Washington, DC 20036

Identification of Reversible Small Molecule Inhibitors of Endothelial Lipase (EL) which Demonstrate HDL-C Increase In Vivo

George Tora,,† Soong-Hoon Kim,† Zulan Pi,† James A. Johnson,† Ji Jiang,† Monique Phillips,† John Lloyd,† Lynn M. Abell,∞ Hao Lu,$ Gregory Locke,£ Leonard P. Adam,‡ David S. Taylor,‡ Xiaohong Yin,‡ Kamelia Behnia,§ Lei Zhao,‡ Richard Yang,‡ Michael Basso,‡ Christian Caporuscio,§ Alice Ye Chen,‡ Eddie Liu,‡ Todd Kirshgessner,‡ Joelle M. Onorato,§ Carol Ryan,‡ Sarah C. Traeger,€ David Gordon,‡ Ruth R. Wexler† and Heather J. Finlay.†*

Departments of Discovery †Chemistry, ‡Biology, ±Pharmaceutics, £Mechanistic Biochemistry, §Pharmaceutical Candidate Optimization, €Discovery Analytical Sciences, Bristol-Myers Squibb, Research and Development, P.O. Box 5400, Princeton, New Jersey 08543-5400, United States

KEYWORDS Endothelial Lipase, HDL, Hepatic Lipase

ABSTRACT: Endothelial lipase (EL) hydrolyzes phospholipids in HDL resulting in reduction in plasma HDL levels. Studies with murine transgenic, KO or loss-of-function variants strongly suggest that inhibition of EL will lead to sustained plasma HDL-C increase and, potentially, a reduced CVD risk. Herein, we describe the discovery of a series of oxadiazole ketones, which upon optimization, led to the identification of Compound **12**. Compound **12** was evaluated in a mouse PD model and demonstrated a 56% increase in plasma HDL-C. In a mouse reverse cholesterol transport study, Compound **12** stimulated cholesterol efflux by 53% demonstrating HDL-C functionality.

INTRODUCTION

Cardiovascular disease (CVD) is the number one cause of mortality globally. An estimated 17.9 million people died from CVD in 2016, representing 31% of all global deaths. Of these, an estimated 85% are due to heart attack and stroke.[1] Coronary heart disease is caused by buildup of plaque in arteries resulting in narrowing of the small blood vessels that supply blood and oxygen to the heart. Every year approximately 735,000 Americans have a heart

attack.[2] In 2016, the total estimated cost, (health care costs, medications and loss in productivity) due to heart disease in the US alone was $555B, with costs expected to reach 1.1 trillion in 2035[3].

Elevated levels of low density lipoprotein cholesterol (LDL-C) are associated with increased atherosclerotic plaque formation and coronary artery disease (CAD)[4]. Reduction of LDL-C has become the cornerstone of treatment to reduce the risk of CV events. Current drug therapy reduces CAD events by 25-30%[5] and there is a further need to reduce events and decrease mortality associated with CAD. It has been shown that high density lipoprotein cholesterol (HDL-C) is an independent risk factor for CAD events and plays a central role in reverse cholesterol transport (RCT). RCT is a process where HDL-C cholesterol is removed from the periphery (e.g., atherosclerotic plaques in blood vessels) to the liver for elimination.[6,7] HDL-C may also serve to reduce blood vessel injury through its antioxidant and anti-inflammatory functions.[8] Recently a phase III study of the cholesterol ester transfer protein (CETP) inhibitor, anacetrapib, did not demonstrate benefit on mortality despite robust increase in HDL-C.[9] It is unclear why elevation of HDL-C through inhibition of CETP was not beneficial, however, evaluation of EL as an alternative mechanism to raise HDL-C could

provide further insight and generate therapeutic agents that may demonstrate cardiovascular benefit.[10,11]

Endothelial lipase is a member of the triglyceride lipase family which includes hepatic lipase, (HL) lipoprotein lipase, (LPL) and pancreatic lipase, (PL).[12] The triglyceride lipase gene family plays a central role in dietary fat absorption. Endothelial lipase is the most recently discovered member of the triglyceride lipase gene family, with 44% structural homology to human LPL and 41% homology to human HL [13,14] Unlike LPL and HL, EL is secreted from vascular endothelial cells and hepatocytes and is believed to function at the site of synthesis to influence plasma HDL-C through phospholipase activity.[15] EL preferentially hydrolyses the SN-1 (PLA_1) ester bond of phosphatidylcholine (PC) present in HDL-C particles, releasing Lyso-PC and ultimately reducing plasma HDL-C and the number of HDL particles that participate in RCT. Studies with murine transgenic, KO or loss-of-function variants demonstrate higher levels of plasma HDL-C. Therefore, [16,17,18] selective inhibition of EL should increase HDL-C and provide a potential benefit in the treatment of cardiovascular disease. Despite the central role that EL plays in HDL-C metabolism, only a few EL inhibitors have been reported.[19,20] The first disclosed small molecule EL inhibitor

(XEN445, **1**, Figure 1) increased HDL-C in WT mice at a plasma concentration of 9.9 μM at 16 h post the last dose.[21] In our hands, this compound did not demonstrate inhibition of EL in serum or plasma based assays. A subsequent disclosure of the irreversible thiocarbamate EL inhibitor (**2**) was reported to increase HDL-C at higher doses of 30 and 100 mg/kg[22]

We have previously disclosed our efforts to identify reversible EL inhibitors with oral bioavailability[23,26-27] (**4** and **5**, Figure 1). Those compounds, however, did not demonstrate elevation in HDL-C in our mouse pharmacodynamic model despite achieving target plasma exposures. Therefore, identification of a selective, reversible EL inhibitor to demonstrate pharmacological proof of concept remained the focus of our effort.

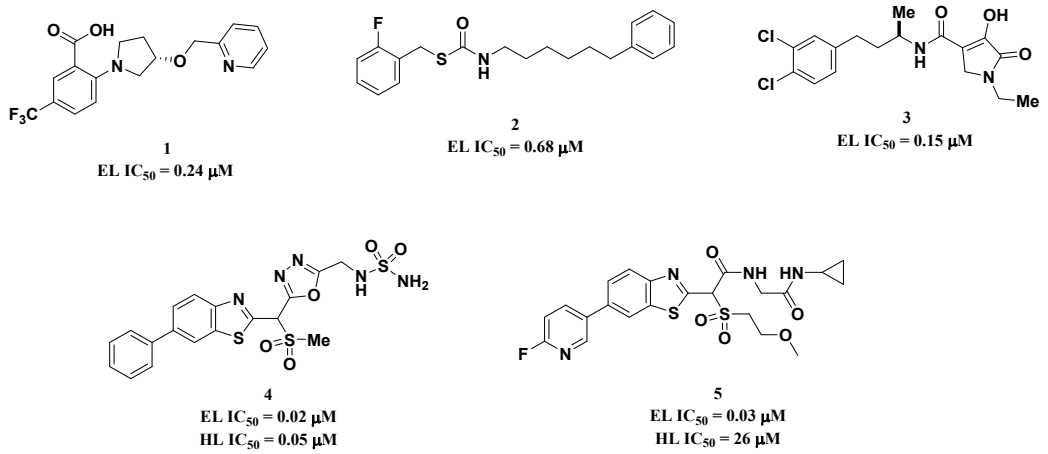

Figure 1. Recently disclosed EL inhibitors

RESULTS

Compound **3** was the first compound advanced to the mouse PD model, (based on potency in a high throughput in vitro vesicle based assay) and demonstrated no effect on HDL-C. This led to the development of a human serum (hSerum) and a mouse plasma assay (mPlasma) as a means to evaluate EL inhibitors in a more biologically relevant environment[23] Subsequent optimization for the in vitro mPlasma potency led to the identification of the EL/HL sulfonated benzothiazole-oxadiazole inhibitor **4.**[26] SAR was further developed concurrent with improving the PK profile resulting in compound **5** which had good hSerum potency (EL IC_{50} 0.12 μM) with acceptable selectivity verses HL (88 fold).[27] Despite compound **3** exhibiting good mouse p.o. PK, with a C_{trough} concentration of >10 fold over mPlasma IC_{50} of 0.12 μM during the course of a 4 day PK/PD study, an increase in HDL-C was, again, not observed.

During the course of our studies to synthesize analogs of **5**, we found that non sulfonated amides like **6** spontaneously oxidized to the keto-amides **7** (Figure 2). This oxidation could be accomplished chemically in both the amide and oxadiazole series, **8** (Figure 2). We sought to establish the stability and reversibility with respect to enzyme activity of these ketones while at the same time maintaining EL activity.

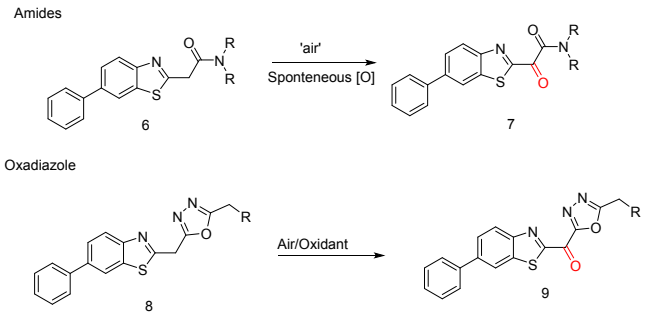

Figure 2. Spontaneous oxidation of amides to keto-amides

Compounds **12-16** were prepared by the general method described in Scheme 1.[26] The methylene bridging the heterocycles was regio-selectively oxidized and the sulfamide deprotected in one pot to give ketones **12-16.** Initially a H_2O_2/AcOH mixture was used to effect this oxidation, but yields were low and the conditions were not tolerant to diverse functional groups. Subsequently, we discovered that using a hypervalent iodine species, [bis(trifluoroacetoxy)iodo]benzene (PIFA) to effect this oxidation resulted in high yields and was more general for selective oxidation in this series.

Table 1. Selectivity versus HL SAR

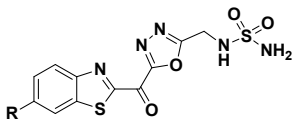

Compound	R	EL (μM)[a]	HL (μM)[a]	EL (μM)[a] human serum	EL (μM)[a] mouse plasma
12		0.005	0.002	0.1	0.06
13		<0.01	0.01	<0.2	<0.2
14		0.03	0.02	0.04	nd[b]
15	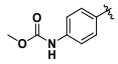	<0.01	0.005	0.4	0.70
16		0.02	0.03	0.8	nd[b]

[a]Inhibition was run at 3 concentrations to calculate IC_{50} values, [b]not determined.

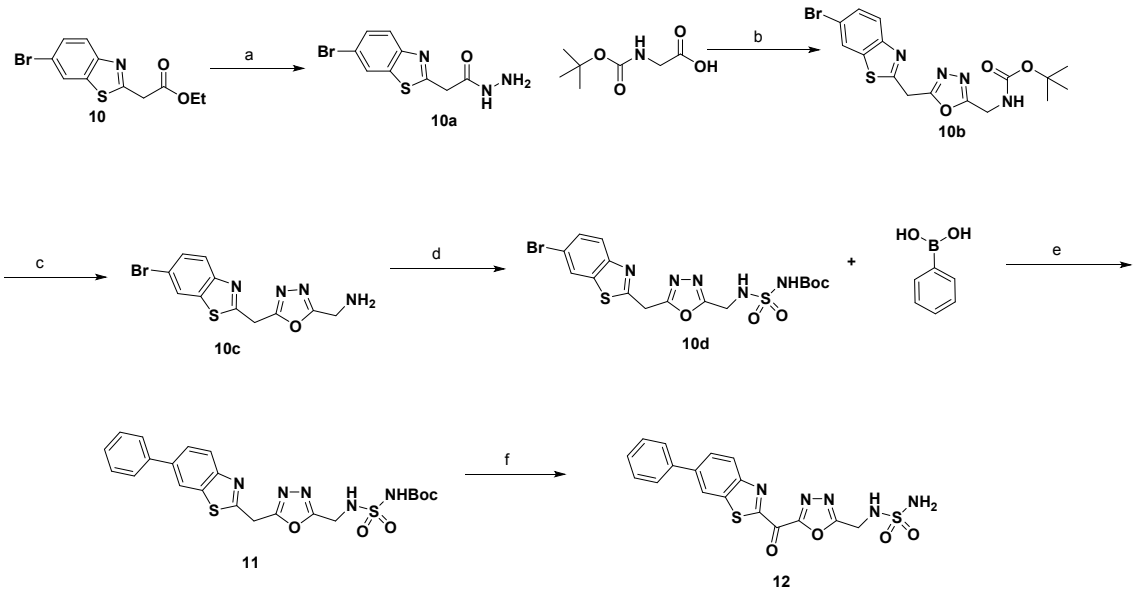

Scheme 1. Reagents and conditions: (a) Hydrazine, EtOH, rt, 94%; (b) T_3P, DIEA, Dioxane, 67%; (c) TFA/ CH_2Cl_2, 100%. (d) N-(tert-butoxycarbonyl)-N-[4-(dimethylazaniumylidene)-1,4-dihydropyridin-1-ylsulfonyl]azanide (N-TDDSA), Pyridine, CH_2Cl_2, 74%; (e) Xphos 2nd Gen., K_3PO_4, THF, 11-62%; (f) PIFA, CH_2Cl_2/H_2O then TFA, 14-50%

The inhibitory activity of compounds for EL and HL was evaluated using a fluorogenic substrate assay. In this assay the lipid hydrolysis was measured in HDL in the presence of overexpressed endogenous human EL from conditioned media obtained from HT-1080 cells. The HL assay was run in the same manner with HL partially purified from conditioned media obtained from COS7 cells. (Table 1). (see supporting information).[23] EL inhibition was also measured in the presence of hSerum and mPlasma. Test compounds were dissolved in DMSO in a 96 well plate and combined with a pre-mixed solution of D31-POPC-HDL/human serum and EL. The plate was incubated at 37 °C for 2 h then quenched with 100% ethanol containing D3-heptadecanoic acid (internal standard). The plate was sealed, centrifuged and transferred to a PCR plate for LC/MS analysis. Ketones **12** to **16** showed improved potency in both the mPlasma and hSerum assays relative to compound **2**, but we did not observe any improvement in selectivity for EL versus HL. Given the excellent EL mouse plasma potency, Compound **12** was chosen as a bench mark compound to evaluate *in vivo*.

We were concerned that the ketone could make a covalent irreversible bond with the enzyme and, as such, compound **12** was evaluated for reversibility. Compound **12** was pre-incubated with the enzyme and then dialyzed. The activity of the enzyme was checked at 24h to determine whether enzyme activity was restored. It was found that at 3 uM, 90% of activity was restored

at 24h and at 9 uM, 64% of activity was restored at 24h, consistent with a competitive mode of inhibition.

Compound **12** was advanced to pharmacokinetic studies to determine exposure (Table 2). The target concentration was >5 fold over the mouse plasma IC_{50} at C_{trough} plasma level. Compound **12** was dosed at 50 mg/kg by p.o., s.c. and i.p. administration (Table 2). When dosed i.p., the 24 h plasma exposure was 9.9 fold over the mouse plasma $IC_{50.}$ Having achieved target exposures, we advanced compound **12** to the mouse pharmacodynamic model to evaluate HDL-C plasma levels.

Table 2. Mouse pharmacokinetic properties[a] for compound **12**

Dosing method	Dose (mg/kg)	Cmax(μM)	C_{24} (μM)	$AUC_{0\text{-}24h}$ (μM.h)
PO[b]	50	10	0.25	48
SC[c]	50	2.9	0.19	21
IP[d]	50	19	0.50	170

[a]Data from fasted, male, C57BL/6 mice (n = 6). [b]Vehicle: EtOH/PEG400/H_2O (10/70/20), [c]Vehicle: EtOH/PEG400/H_2O (10/60/30), [d]Vehicle: 2% PVP-K/0.15%SLS/97.85% H_2O, dosed as a nano suspension

Compound **12** was dosed at 50 mg/kg, *i.p.* QD in wild type mice (n=6) for 2 days. Mice were fasted 5 hours prior to bleed on day minus 1 and the first dose administered 18 h post bleed

with the final dose administered 24 h after the first dose. 1 h post the second dose, the mice were fasted for 5 h and blood samples collected at 30 h post initial dose (6 h post final dose). A 56% elevation in plasma HDL-C concentration was observed at 30 hours (6 hours post last dose). The plasma concentration was 520 ± 0.32 nM consistent with previous PK studies (Figure 4).

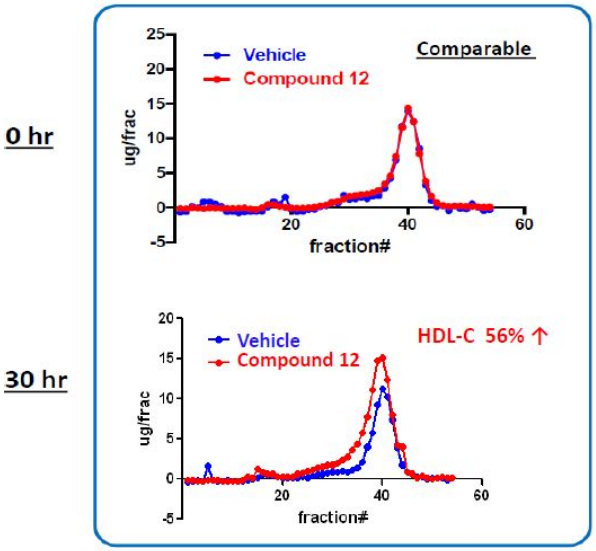

Figure 4: HDL-C elevation with compound **12** *i.p., QD* adminstration at 30 hours post first dose, (6 hours post second dose).

It was encouraging to observe robust, and exposure-dependent, elevation of HDL-C in this model. To demonstrate that the HDL-C elevation was due to on-target EL inhibition, a PD study (50 mg/kg, *i.p*, *BID*) in HL KO and EL KO mice was undertaken (Figure 5). Mice were fasted 5 hours prior to baseline bleed on day minus 1. Three doses were administered with the final dose

administered at 24 h after the first dose. 1 h post third dose, the mice were fasted for 5 h and blood samples collected at 30 h post initial dose (6 h post final dose). In the HL KO PD study, a 32% elevation of HDL was observed at 30 hours, at a plasma concentration of 11.0 ± 7.4 μM. In the EL knockout PD study no elevation of HDL was observed at a plasma concentration of 8.5 ± 1.1 μM. These studies showed that the HDL-C elevation observed in wild type mice was due to EL inhibition and not due to HL inhibition. Sustained HDL-C increase by compound **12** in WT and KO HL mouse is consistent with EL inhibition as the mechanism for HDL-C elevation.

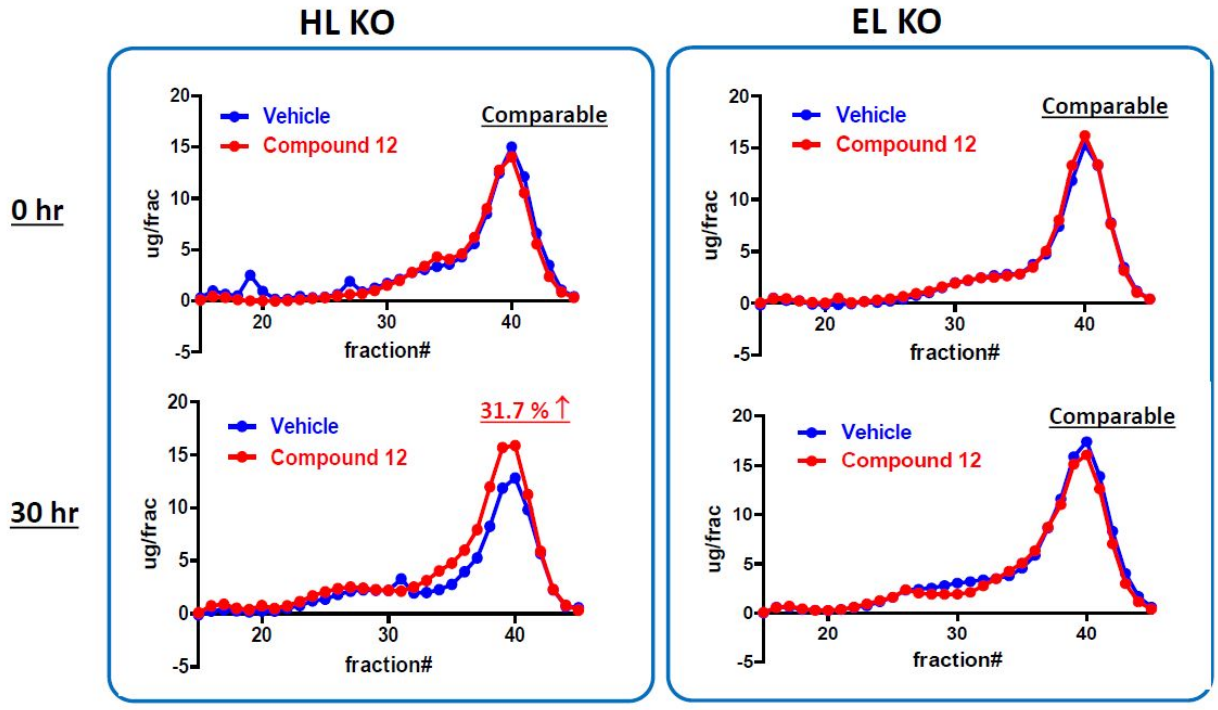

Figure 5: HL and EL knock out PD study

Unlike humans, wild type mice have a relatively high level of HDL-C concentration and low levels of LDL-C. In the dual transgenic *h*CETP/apoB-100 mouse, the lipid profile more closely resembles that of humans. Compound **12** elevated HDL-C by 36% when dosed at 50 mg/kg, *i.p.,* BID in the dual transgenic mice and did not affect the LDL-C level.

It has also been shown that HDL-C plays a central role in RCT, a multi-step process resulting in the net movement of cholesterol from peripheral tissues back to the liver.[7] Cellular cholesterol efflux is mediated by HDL-C, acting in conjunction with the enzyme lecithin:cholesterol acyltransferase (LCAT). In a RCT WT mouse model,[24-25] mice (n=3) were dosed with compound **12** at 50 mg/kg, *i.p,* QD, followed by i.v administration of ^{3}H-labelled cholesterol on day 3 (Figure 6). The labelled particles were rapidly taken up by macrophages in the reticuloendothelium system (RES). The nadir of this initial clearance phase was observed 15-30 minutes post injection (Figure 6). The reappearance of label after 30 minutes represents the efflux of cholesterol out of the RES macrophages onto circulating HDL. Therefore, the macrophage specific efflux was due to the formulation of 3H-cholesterol tracer (albumin complexed nanoparticles) and the manner in which these particles are distributed following i.v adminstration. The net movement of ^{3}H-labelled cholesterol back to the plasma compartment

was measured over 2.5 hours. In this experiment, compound **12** stimulated cholesterol efflux by 53% demonstrating HDL-C functionality.

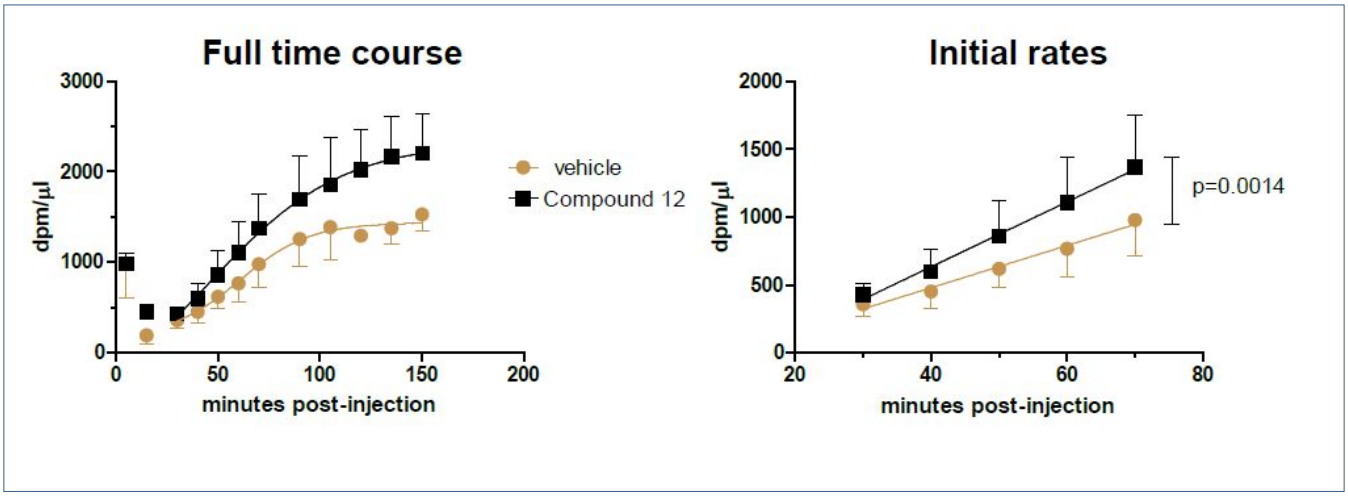

Figure 6. Compound **12** stimulates Macrophage Cholesterol Efflux. Initial cholesterol efflux rates determined by linear regression and two-tailed p values for differences in slopes between the treatment groups calculated (Graphpad Prism, 5.01)

As the physiological effect of HL inhibition is not well understood, we continued our search for a compound with an improved selectivity profile with respect to HL and an improved oral PK profile. We chose to substitute the sulfamide with other functional groups in an effort to improve HL selectivity and ADME properties.

Compound **21** was generated as shown in Scheme 2 from sulfur isocyanatidic chloride, which was acylated with 2-chloroethanol and condensed with compound **17** to afford intermediate

oxazolidine **18**. Compound **18**, a versatile intermediate, was converted to various alkylsulfamides, for example, compound **19** in 69% yield. XPhos 2nd Gen mediated Suzuki coupling followed by selective oxidation afforded **21** in 24-50% yields. Compounds **22-24** were synthesized by the general route shown in Scheme 2.

Scheme 2.

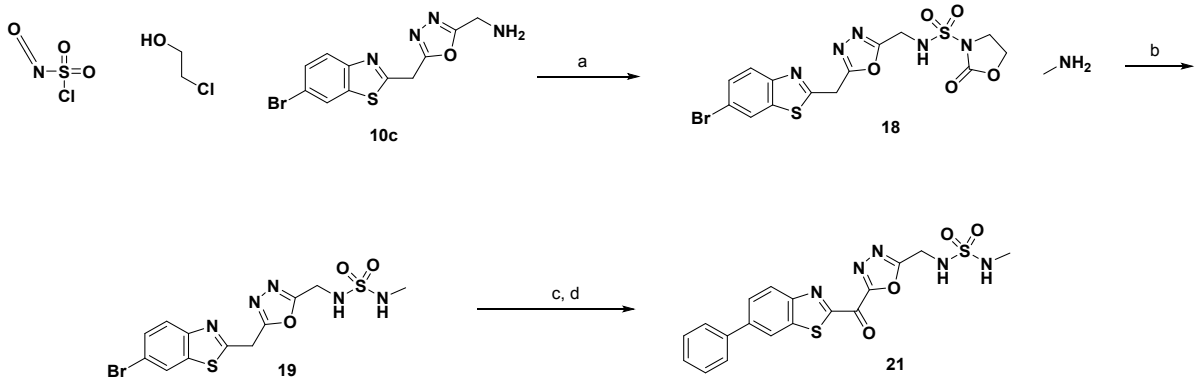

Scheme 2. Reagents and conditions: (a) TEA, CH_2Cl_2, rt, 73%; (b) TEA, ACN, 95ºC, 69%; (c) Xphos 2nd. Gen., K_3PO_4, THF, 22-68%; (d) PIFA, CH_2Cl_2/H_2O then TFA, 5-50%.

Scheme 3.

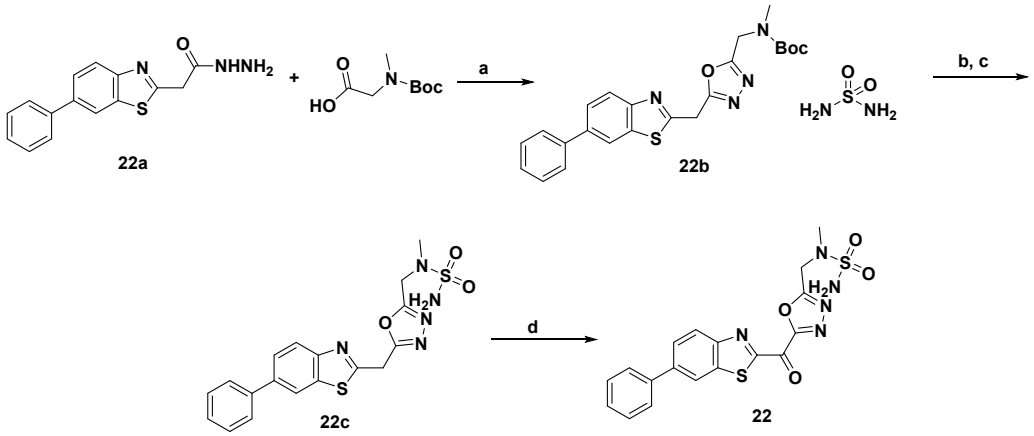

Scheme 3. Reagents and conditions: (a) T_3P, DIEA, Dioxane, 19%; (b) TFA/DCM (c) 1,4-dioxane, 100 °C, 53%; (d)H_2O_2/AcOH, 21%

Scheme 4.

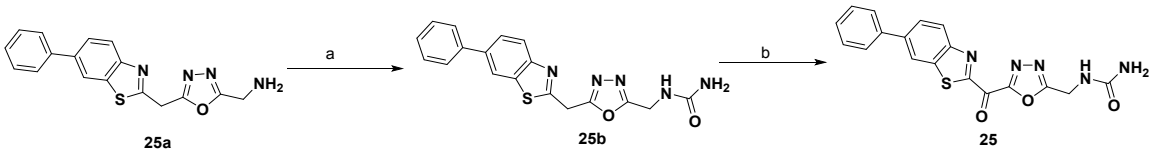

Scheme 4. Reagents and conditions: (a) KOCN,AcOH/H_2O, rt, 31%; (b) H_2O_2, AcOH, 23%.

Substitution of the terminal nitrogen with a methyl resulted in compound **21** which had EL hSerum potency of 140 nM, but no selectivity against HL. This primary sulfamide was the most potent compound in this series and we focused on further optimization of **12**. Substitution of the internal nitrogen with a methyl group resulted in a loss of EL hSerum potency (**22**). There was no improvement in potency by substituting the α-position with a methyl. Both the S and R methyl substitutions (**23** and **24**) resulted in 30-100 fold loss in potency as compared to **12**. The corresponding urea analogue, compound **25**, was also prepared (Scheme 3) but was less potent in the EL hSerum assay and showed no improvement in HL selectivity. Having realized no selectivity improvement as a result of SAR on the sulfamide, we sought to keep the primary sulfamide constant and explore SAR at the C5 and C6 positions.

Table 3. Sulfamide SAR

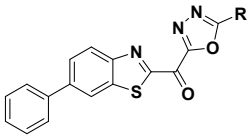

Compound	R	EL (μM)[b]	HL (μM)[b]	EL (μM)[b] human serum	EL (μM)[b] mouse plasma
21	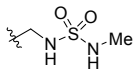	0.02	0.01	0.1	nd[e]
22[a]	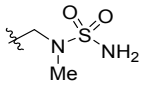	0.02	0.003	7	1
23[a]	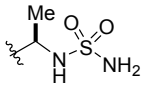	0.09	0.06	2	0.2
24[a]	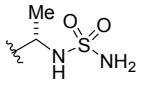	0.2	0.03	10	3
25	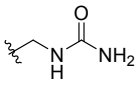	0.03	>0.01	1	1

[b]Inhibition was run at 3 concentrations to calculate IC_{50} values.

Previously disclosed SAR[26] on benzothiazole–linked sulfones showed that selectivity could be improved by incorporating polar aryl substituents at C-6. However, the strategy to replace the

phenyl group with 4-fluoro pyridyl, (**14**) in the ketone series was unsuccessful. Subsequently, we sought to modify the electronics of the benzothiazole core to improve selectivity by incorporating fluorine at C5 and C6. Combining polarity at C6 with fluorine substitution at C5, gave compound **28** (Table 4), which maintained EL activity with a modest increase in selectivity versus HL, (9 fold). We synthesized additional C6 substituted compounds with C5 fluorine substitution (Table 4) and observed an increase in selectivity over HL while maintaining the EL hSerum potency as shown by compound **29 and 30,** (EL hSerum potency of 0.06 uM and 0.02 uM, EL selectivity **38** and **41** fold respectively). Less polar amide, compound **31** had reduced EL selectivity (8 fold). Similar SAR was observed by reversing the substitution of polar substituent at C5 and fluorine substitution at C6 (**32 and 33**). To further evaluate our compounds and prioritize for mouse PK, compounds were tested in HL KO mPlasma assays. Compounds which had better HL KO mPlasma activity together with improved EL selectivity were progressed to mouse PK. Compound **32** (EL hSerum potency of 0.04 uM, EL selectivity of >32, HL KO mPlasma IC_{50} of 0.2 μM and excellent human, rat and mouse liver microsome stability) was selected in the C-6 Fluoro series. In the C5 fluoro series, compound **31** (EL hSerum potency of 0.04 μM, EL selectivity of >9, HL KO mPlasma IC_{50} of 0.2 μM and >80% liver microsome stability

in human, rat and mouse) was advanced to rat PK studies with **32** (Table 4). Both compounds showed good exposure on i.p. QD dosing (Table 5): compound **31** (C_{max} = 7.1 μM, C_{24} = 0.26 μM, AUC = 58.0 μM*h at 50 mg/kg) and compound **32** (C_{max} = 21.0 μM, C_{24} = 0.46 μM, AUC = 36.0 μM*h at 50 mg/kg). Hence, both compounds **31** and **32** were advanced to a mouse PD study.

Table 4: C5 and C6 Fluoro effect on selectivity versus HL

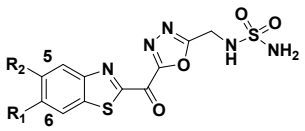

Compound	R_1	R_2	EL (μM)[b]	HL (μM)[b]	EL (μM) human serum	HL KO IC_{50} (μM)[a]	Met Stab H/M[b]
14		H	0.03	0.02	0.04	nd	78/68
28		F	0.001	0.009	0.02	nd	--/66

29		F	0.0005	0.02	0.06	0.2	81/--
30		F	0.0009	0.04	0.02	nd	80/-
31	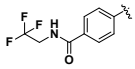	F	<0.0005	0.004	0.05	0.2	87/--
32	F		<0.0005	0.02	0.04	0.2	96/100
33	F	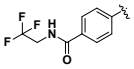	<0.0005	0.004	0.2	0.2	98/100

[a]Inhibition was run at 3 concentrations to calculate IC_{50} values. [b]Percentage of compound (0.5 uM) remaining after 10 minute incubation in human, rat and mouse liver microsomes.

Table 5. Mouse *i.p.* PK properties[a]

Compound	Dose (mg/kg)	C_{max}(μM)	C_{min} (μM)	$AUC_{0\text{-}24h}$ (μM.h)
31[b]	50[c]	7.1	0.25	58
32[b]	50[c]	21	0.46	36

[a]data from fasted, male, C57BL/6 mice (n = 6), [b]Vehicle: 2% PVP-K/0.15% SLS/97.85% H_2O. [c]Dosed as a nano suspension

Wild-type C57BL/6 mice (n = 6) were dosed with compounds **31** and **32** at 50 mg/kg i.p. QD. Separately, a set of mice (n = 3) were dosed as per protocol and utilized to determine

plasma exposure at 24 h. This satellite group showed a lower than projected exposure (target coverage: 5X mouse IC_{50} at C_{trough}) at 24 h (**32**:C24h = 96 nM, 4.8X lower and **31**: C24h = 36 nM, 7.2X lower). The lipid profile was measured using FPLC analysis of blood samples taken at 30h (6h post final dose) and showed a 38% and 37% increase in HDL-C concentrations for compounds **31** and **32** respectively.

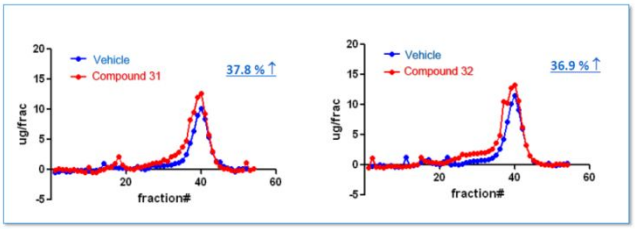

Figure 5: HDL-C elevation with compound **31** and **32** following *i.p.* QD administration.

DISCUSSION AND CONCLUSION

In summary, we have identified small molecule, reversible EL inhibitors which demonstrated a significant elevation of HDL-C in a WT-mouse PD model. We have also shown that dual EL-HL inhibitor, **12,** raised HDL-C in WT and HL KO mice but had no effect on EL KO mice demonstrating that HDL-C increase is due to EL inhibition. Compound **12** demonstrated increased reverse cholesterol transport in mouse in addition to causing a sustained and exposure related plasma HDL-C elevation in mice, thus

demonstrating functionality of the elevated HDL. In addition, we have identified compounds with potency for EL and increased selectivity versus HL, which demonstrated increased HDL-C in the mouse PD model (compounds **31** and **32**).

EXPERIMENTAL SECTION

Chemistry: General Methods. All solvents and reagents were used as obtained. Reactions involving air or moisture sensitive reagents were carried out under argon atmosphere. Microwave reactions were performed using Biotage® Initiator reactors. NMR spectra were recorded in a deuterated solvent with a Bruker or JEOL® Fourier transform spectrometers operating at frequencies as follows: ^{1}H NMR: 400 MHz (Bruker or JEOL®) or 500 MHz (JEOL®). ^{13}C NMR: 100 MHz or 125 MHz (Bruker). Spectra data are reported in the format: chemical shift (multiplicity, coupling constants, number of hydrogens). Chemical shifts are specified in ppm downfield of a tetramethylsilane internal standard (δ units, tetramethylsilane = 0 ppm) and/or referenced to solvent peaks, which in ^{1}H NMR spectra appear at 2.49 ppm for CD_2HSOCD_3, 3.30 ppm for CD_2HOD, and 7.24 ppm for $CHCl_3$, and which in ^{13}C NMR spectra appear at 39.7 ppm for CD_3SOCD_3. All ^{13}C NMR spectra were proton decoupled. All coupling constants (J) are reported in Hertz.

LCMS chromatograms were obtained on a Shimadzu HPLC system running Discovery VP software, coupled with a Waters® Micromass ZQ mass spectrometer running MassLynx version 3.5 software and using the following methods. For each method the LC column was maintained at room temperature and UV detection was set to 220 nm. Analytical purity was >95% unless stated otherwise.

Method B: A linear gradient using solvent A (10% methanol, 90% water, 0.1% of TFA) and solvent B (90% methanol, 10% water, 0.1% of TFA); 0-100% of solvent B over 2 min and then 100% of solvent B over 1 min. Column: PHENOMENEX® Luna 5 μm C18 (2.0 x 30 mm). Flow rate was 1 mL/min.

Method M: A linear gradient using of Solvent A (0.05% TFA, 100% water) and Solvent B (0.05% TFA, 100% ACN); 2 to 98% B over 1 min, with 0.5 min hold time at 98% B. Column: Waters BEH C18 (2.1 x 50 mm). Flow rate: 0.8 mL/min.

2-(6-Bromobenzo[d]thiazol-2-yl)acetohydrazide (10a): Ethyl 2-(6-bromobenzo[d]thiazol-2-yl)acetate (3.0 g, 10.0mmol) was combined with hydrazine (3.14 mL, 100 mmol) in methanol (60 mL) and stirred at room temperature. After 16 h, a precipitate formed that was collected by filtration and washed with ethyl acetate (2X) to afford compound **7** (2.7 g, 94%) as a white solid. LC/MS *m/z* = 288.0 [M+H], RT = 0.68 min (Method M). MS (ES). ^{1}H NMR (500 MHz, DMSO-d_6) δ 9.47 (br s, 1H), 8.37 (d, *J*=2.2 Hz, 1H), 7.89 (d, *J*=8.8 Hz, 1H), 7.64 (dd, *J*=8.7, 2.1 Hz, 1H), 4.36 (br d, *J*=3.9 Hz, 2H), 3.99 (s, 2H)

***tert*-Butyl ((5-((6-bromobenzo[d]thiazol-2-yl)methyl)-1,3,4-oxadiazol-2-yl)methyl)carbamate (10b):** Compound **10a** (400 mg, 1.40 mmol) and 2-((tert-butoxycarbonyl)amino)acetic acid (294 mg, 1.68 mmol) were dissolved in dioxane (10 mL) and

treated with 1-propanephosphonic acid cyclic anhydride (2.08 mL, 3.49 mmol) (50% in ethyl acetate) and DIEA (0.610 mL, 3.49 mmol). The reaction mixture was heated at 70°C. After 1 h, the reaction was allowed to cool to rt and treated with additional 1-propanephosphonic acid cyclic anhydride (2.08 mL, 3.49 mmol) (50% in ethyl acetate) and DIEA (0.610 mL, 3.49 mmol). The reaction mixture was stirred at 105 °C for 16 h. After allowing to cool to rt, the reaction was concentrated under reduced pressure and the residue was purified on ISCO (0-100% Hex/EtOAc) to afford compound **10b** (400 mg, 67%). LC/MS *m/z* = 427.1 (M+H). RT = 1.91 min (Method B). ^{1}H NMR (500 MHz, CHLOROFORM-d) δ 7.83 (dd, *J*=1.7, 0.8 Hz, 1H), 7.41 (d, *J*=1.7 Hz, 1H), 7.39 (d, *J*=1.9 Hz, 1H), 4.76 (s, 2H), 4.59 (d, *J*=5.0 Hz, 2H), 1.47 (s, 9H)

(5-((6-Bromobenzo[d]thiazol-2-yl)methyl)-1,3,4-oxadiazol-2-yl)methanamine (10c): Compound **10b** (300 mg, 0.677 mmol) was combined with DCM (4.0 mL) and treated with TFA (4.0 mL) at room temperarure for 30 min. The solvents were evaporated under reduced pressure and azeotroped with toluene (3X). The resulting white solid was dissolved in DCM and washed with phosphate buffer (1.5 M), brine, dried over sodium sulfate, filtered and concentrated under reduced pressure to afford compound **10c** (260 mg, *quant.*) which was used as is in the next step. LC/MS *m/z* = 327.0 (M+H). RT = 1.34 min (Method B).

***tert*-Butyl (N-((5-((6-bromobenzo[d]thiazol-2-yl)methyl)-1,3,4-oxadiazol-2-yl)methyl)sulfamoyl)carbamate (10d):** To a solution of compound **10c** (220 mg, 0.640 mmol) in DCM (10 mL) and pyridine (0.520 mL, 6.40 mmol) was added (tert-butoxycarbonyl)((4-(dimethyliminio)pyridin-1(4H)-yl)sulfonyl)amide (203 mg, 0.673 mmol). After 16 h, the reaction

mixture was evaporated under reduced pressure to dryness, dissolved in EtOAc and poured into satd NH_4Cl. The aqueous portion was extracted with EtOAc (3X) and the combined organic extracts were washed with brine, dried over sodium sulfate, filtered and concentrated under reduced pressure. The residue was purified on ISCO (0 to 100% EtOAc/DCM) to give compound **10d** (246 mg, 74%) as a white solid. LC/MS *m/z* = 505.9 (M+H). RT = 1.82 min (Method B). ^{1}H NMR (400 MHz, CHLOROFORM-d) δ 7.95 (d, *J*=2.0 Hz, 1H), 7.80 (d, *J*=8.5 Hz, 1H), 7.54 (dd, *J*=8.8, 2.0 Hz, 1H), 4.66 (s, 2H), 4.47 (s, 2H), 1.30 (s, 9H)

***tert*-Butyl (N-((5-((6-phenylbenzo[d]thiazol-2-yl)methyl)-1,3,4-oxadiazol-2-yl)methyl)sulfamoyl)carbamate (11):** To a solution of Compound **10d** (110 mg, 0.210 mmol) and phenylboronic acid (38.5 mg, 0.320 mmol) in dioxane (2 mL) and water (0.5 mL) was added potassium phophate (112 mg, 0.530 mmol), and 2nd Gen. Xphos precatalyst (16.57 mg, 0.020 mmol). The mixture was degassed by purging reaction mixture with argon and heated at 90 °C for 2 h. After allowing to cool to room temperature, the reaction mixture was filtered and concentrated under reduced pressure. The residue was purified on ISCO (0-15% DCM/Methanol) to afford compound **11** (52 mg, 48%) as a light brown solid. LC/MS *m/z* = 501.9 [M+H], RT = 1.96 min (Method B).

N-((5-((6-Phenyl-1,3-benzothiazol-2-yl)carbonyl)-1,3,4-oxadiazol-2-yl)methyl)sulfamide (12). To a solution of compound **11** (117 mg, 0.290 mmol) in CH_2Cl_2 (5 mL), TFA (0.1 mL) and water (26 µL, 1.5 mmol) was added [bis(trifluoroacetoxy)iodo]benzene (376 mg, 0.870 mmol) at room tempeartue. The mixture mixture was stirred for 10 min and concentrated under reduced pressure. The residue was purified on ISCO (0-10% DCM/Methanol) to afford compound **12** (21 mg, 18%) as a yellow solid. LC/MS *m/z* = 416.3 (M+H). RT = 1.81 min (Method B). HRMS *m/z* (ESI) calcd for $C_{17}H_{13}N_5O_4S_2$ ($[M+H]^+$) 416.0482, found 416.0467. ^{1}H NMR (500MHz,

ACETONITRILE-d_3) δ 8.44 (d, *J*=1.3 Hz, 1H), 8.37 (d, *J*=8.5 Hz, 1H), 8.00 (dd, *J*=8.7, 1.7 Hz, 1H), 7.80 - 7.78 (m, 2H), 7.56 - 7.53 (m, 2H), 7.46 (m, 1H), 6.01 (br t, *J*=5.5 Hz, 1H), 5.60 - 5.34 (m, 2H), 4.61 (s, 2H). ^{13}C NMR (126MHz, ACETONITRILE-d_3) δ 172.1, 167.6, 163.5, 162.0, 154.2, 143.2, 140.9, 139.6, 130.6 (s, 2C), 129.8, 128.9, 128.8 (s, 2C), 127.5, 122.1, 39.2.

Compounds **31 and 32** were prepared from **10d** using the methods and conditions described for **12**

4-(5-Fluoro-2-{5-[(sulfamoylamino)methyl]-1,3,4-oxadiazole-2-carbonyl}-1,3-benzothiazol-6-yl)-N-(2,2,2-trifluoroethyl)benzamide (31). 26% yield. LCMS (method M) retention time = 0.75 min, $(M+H)^+$ = 559.0. HRMS *m/z* (ESI) calcd for $C_{20}H_{14}F_4N_6O_5S_2$ ($[M-H]^-$) 557.0319, found 557.0332. ^{1}H NMR (500 MHz, Acetone-d6) δ 8.51 (d, *J*=7.3 Hz, 1H), 8.44 (t, *J*=6.3 Hz, 1H), 8.19 (d, *J*=11.0 Hz, 1H), 8.11 (d, *J*=8.5 Hz, 2H), 7.84 (dd, *J*=8.2, 1.6 Hz, 2H), 6.85 (t, *J*=5.8 Hz, 1H), 6.27 (s, 2H), 4.75 (d, *J*=6.0 Hz, 2H), 4.23 (qd, *J*=9.5, 6.6 Hz, 2H). ^{13}C NMR (126 MHz, Acetone-d6) δ 171.3, 167.6, 167.5, 165.4, 161.6, 160.5 (d, *J*=247.0 Hz, 1C), 154.8 (d, *J*=12.7 Hz, 1C), 139.2, 134.8 (d, *J*=1.8 Hz, 1C), 134.7, 131.5 (d, *J*=17.3 Hz, 2C), 130.4 (d, *J*=2.7 Hz, 1C), 128.8 (s, 2C), 125.4 (d, *J*=4.5 Hz, 1C), 125.9 (q, *J*=278.8 Hz, 1C), 112.7 (d, *J*=25.4 Hz, 1C), 41.5 (q, *J*=34.5 Hz, 1C), 39.0. ^{19}F NMR (471 MHz, Acetone-d6) δ -72.70 (t, *J*=9.5 Hz, 3F), -117.94 (t, *J*=8.7 Hz, 1F).

N-({5-[6-Fluoro-5-(1-oxo-2,3-dihydro-1H-isoindol-5-yl)-1,3-benzothiazole-2-carbonyl]-1,3,4-oxadiazol-2-yl}methyl)aminosulfonamide (32). 34% yield. LCMS (method E) retention time = 0.73 min, $(M+H)^+$ = 489.0. HRMS *m/z* (ESI) calcd for $C_{27}H_{26}N_6O_6ClS_3$ ($[M-H]^-$) 487.0289, found 487.0302. ^{1}H NMR (500 MHz, DMF-d7) δ 8.57 - 8.56 (m, 1H), 8.56 - 8.55 (m,

1H), 8.46 (d, *J*=10.1 Hz, 1H), 7.98 (s, 1H), 7.92 - 7.89 (m, 1H), 7.89 - 7.86 (m, 1H), 7.71 (br t, *J*=6.1 Hz, 1H), 6.98 (s, 2H), 4.75 (d, *J*=6.0 Hz, 2H), 4.60 (s, 2H). ^{13}C NMR (126 MHz, DMF-d7) δ 170.4, 170.0, 167.3, 161.1, 159.4 (d, *J*=250.7 Hz, 1C), 150.9, 145.3, 138.5 (br d, *J*=12.7 Hz, 1C), 138.1, 133.3, 132.1, 130.5 (br d, *J*=17.3 Hz, 1C), 129.4 (br d, *J*=2.7 Hz, 1C), 127.9 (br d, *J*=4.5 Hz, 1C), 125.1 (br d, *J*=2.7 Hz, 1C), 123.4, 110.3 (br d, *J*=30.0 Hz, 1C), 45.6, 38.2. ^{19}F NMR (471 MHz, DMF-d7) δ -114.74 (br t, *J*=8.7 Hz, 1F). Orthogonal HPLC purity: Method O1: RT = 5.02 min, 96%; Method O2: RT = 5.86 min, 99%.

ASSOCIATED CONTENT

Supporting Information.

The supporting information is available free of charge at

Experimental details on chemistry general methods; experimental section; biological activity; revesibility assays and reversibility study for compound **12**; standard deviations of EL IC_{50}, HL IC_{50} and EL hSerum IC_{50} for compounds **12**, **31** and **32;** pharmacokinetics**,** single-dose mouse pharmacokinetics and mouse PD studies; Molecular formula strings(CSV)

AUTHOR INFORMATION

Corresponding Author

E-mail: george.tora@bms.com.

Present Address

§(K.B) Glaxosmithkline PRR DPU, 1250 S Collegeville Rd, Collegeville, PA 19426, United States.

∞(L.A.) Agios Pharmaceuticals, 88 Sidney Street, Cambridge MA 02139, United States.

‡(R.Y.) Sollers Institute, 55 Parsonage Road, Edison NJ 08837, United States.

$(H.L.) EMD Serono Research and Development, 45 Middlesex Turnpike, Billerica, MS 01821, United States.

Author Contributions

All authors have given approval to the final version of the manuscript.

Notes

The authors were employed by Bristol-Myers Squibb at the time of this work and some authors may own stock.

ACKNOWLEDGMENT

The authors would like to thank Dr. Arvind Mathur, Rick Rampulla and colleagues at Department of Discovery Synthesis at Biocon Bristol-Myers Squibb RD Center for the preparation of intermediates.

ABBREVIATIONS

HDL, high density lipoprotein; HDL-C, high density lipoprotein cholesterol; KO, knock-out; SAR, structure activity relationship, CVD, cardiovascular disease; EL, endothelial lipase; HL, hepatic lipase; LPL, lipoprotein lipase; PK, pharmokinetic; PD,

pharmacodynamic; FPLC, fast protein liquid chromatography; N-TDDSA, *N*-(tert-butoxycarbonyl)-*N*-[4-(dimethylazaniumylidene)-1,4-dihydropyridin-1-ylsulfonyl]azanide BID, dosing twice daily, QD, dosing once daily; H_2O_2, Hydrogen peroxide; AcOH, acetic acid; PIFA, [bis(trifluoroacetoxy)iodo]benzene.

REFERENCES

1. World Health Organization. Fact sheet. *Cardiovascular diseases (CVDs)*. 17 May **2017**.
2. Mozaffarian D, Benjamin, E. J.; Go, A. S.; Arnett, D, K.; Blaha, M. J.; Cushman, M.; de Ferranti, S.; Després, J. P.; Fullerton, H. J.; Howard, V. J.; Huffman, M. D.; Judd, S. E.; Kissela, B. M.; Lackland, D. T.; Lichtman, J. H.; Lisabeth, L. D.; Liu, S.; Mackey, R. H.; Matchar, D. B.; McGuire, D. K.; Mohler, E. R 3rd.; Moy, C. S.; Muntner, P.; Mussolino, M. E.; Nasir, K.; Neumar, R. W.; Nichol, G.; Palaniappan, L.; Pandey, D. K.; Reeves, M. J.; Rodriguez, C. J.; Sorlie, P. D.; Stein, J.; Towfighi, A.; Turan, T. N.; Virani, S. S.; Willey, J. Z.; Woo, D.; Yeh, R. W.; Turner, M. B.. Heart disease and stroke statistics—2015 update: a report from the American Heart Association. *Circulation*. **2015**;131:e29-322.
3. American Heart Association 1/17DS11775, **2017**
4. (a) Martinez, L. O.; Jacquet, S.; Tercé, F.; Collet, X.; Perret, B.; Barbaras, R. New insight on the molecular mechanisms of high-density lipoprotein cellular interactions. *Cell. Mol. Life Sci.* **2004,** *61* (18), 2343-2360; (b) Gordon, D. J.; Probstfield, J. L.; Garrison, R. J.; Neaton, J. D.; Castelli, W. P.; Knoke, J. D.; Jacobs, D. R., Jr.; Bangdiwala, S.; Tyroler, H. A. High-density lipoprotein cholesterol and cardiovascular disease. Four prospective American studies. *Circulation* **1989,** *79* (1), 8-15
5. Khera, A. V.; Cuchel, M.; Llera-Moya, M.; Rodriques, A.; Burke, M.; Jafri, K.; French, B. C.; Phillips, J. A.; Mucksavage, M. L.; Wilensky, R. L.; Mohler, E. R.; Rothblat, G. H.; Rader, D. Cholesterol efflux capacity, high-density lipoprotein function, and atherosclerosis. J. *N. Engl. J. Med*. **2011**, 364, 127-135.
6. Gordon, T.; Castelli, W. P.; Hjortland, M. C.; Kannel, W. B.; Dawber, T. R. High density lipoprotein as a protective factor against coronary heart disease. The Framingham study. *J. Am. Med*. **1977**, 707-714.
7. Annema, W.; Tietge, U. J. Role of hepatic lipase and endothelial lipase in high-density lipoprotein-mediated reverse cholesterol transport. *Curr. Atheroscler. Rep* **2011**, *13*, 257-265.
8. Soran, H.; Hama, S.; Yadav, R.; Durrington, P. N. HDL functionality. *Curr. Opin. Lipidol*. **2012**, 23 (4), 353-366.
9. Filippatos, T. D.; Kei, A.; Elisaf, M. S. Anacetrapib, a New CETP Inhibitor: The New Tool for the Management of Dislypidemias? Diseases 2017, 5, 21.
10. Hafiane, A.; Genest, J. HDL, Atherosclerosis, and Emerging Therapies. Cholesterol 2013, 2013, 1−18.
11. DeSantis, P.; Coleman, T.; Schiekofer, S.; Nawroth, P. P.; Schlimmer, P.; Schneider, J. G. Mini-Rev. Med. Chem. 2008, 8, 619-627.
12. Jaye, M.; Lynch, K. J.; Krawiec, J.; Marchadier, D.; Maugeais, C.; Doan, K.; South, V.; Amin, D.; Perrone, M.; Rader, D. J. A novel endothelial-derived lipase that modulates HDL metabolism. *Nat. Genet.* **1999,** *21* (4), 424-428.
13. Hirata, K.; Dichek, H. L.; Cioffi, J. A.; Choi, S. Y.; Leeper, N. J.; Quintana, L.; Kronmal, G. S.; Cooper, A. D.; Quertermous, T. Cloning of a unique lipase from endothelial cells extends the lipase gene family. *J. Biol. Chem*. **1999**, 274, 14170-14175.
14. Jaye, M.; Lynch, K. J.; Krawiec, J.; Marchadier, D.; Maugeais, C.; Doan, K.; South, V.; Amin, D.; Perrone, M.; Rader, D. A novel endothelial-derived lipase that modulates HDL metabolism. *J. Nat. Genet*. **1999**, 21, 424-428.
15. Choi, S. Y.; Hirata, K.; Leo, G. C.; Ishida, T.; Quertermous, T.; Cooper, A. D. Endothelial lipase: a new lipase on the block. *J. Lipid Res.* **2002**, *43*, 1763-1769.

16. Ishida, T.; Choi, S. Y.; Kundu, R. K.; Spin, J.; Yamashita, T.; Hirata, K.; Kojima, Y.; Yokoyama, M.; Cooper, A. D.; Quertermous, T. Endothelial lipase modulates susceptibility to atherosclerosis in apolipoprotein-E-deficient mice. *J. Biol. Chem*. **2004**, 279, 45085-45092.
17. Ishida, T.; Choi, S. Y.; Ramendra, K.; Kundu, R. K.; Hirata, K.; Rubin, E. M.; Cooper, A. D.; Quertermous, T. Endothelial lipase is a major determinant of HDL level. *J. Clin Invest*. **2003**, 111, 347-355.
18. Edmondson, A. C.; Braund, P. S.; Stylianou, I. M.; Khera, A. V.; Nelson, C. P.; Wolfe, M. L.; DerOhannessian, S. L.; Keating, B. J.; Qu, L.; He, J.; Tobin, M. D.; Tomaszewski, M.; Baumert, J.; Klopp, N.; Döring, A.; Thorand, B.; Li, M.; Reilly, M. P.; Koenig, W.; Samani, N. J.; Rader, D. J. Dense genotyping of candidate gene loci identifies variants associated with high-density lipoprotein cholesterol. *Circ. Cardiovasc. Genet.* **2011,** *4* (2), 145-155.
19. Brown, R. J.; Lagor, W. R.; Sankaranaravanan, S.; Yasuda, T.; Quertermous, T.; Rothblat, G. H.; Rader, D. *J.* Impact of combined deficiency of hepatic Lipase and endothelial lipase on the metabolism of both high-density lipoproteins and apolipoprotein B–containing lipoproteins. *Circ. Res*. **2010**, 107, 357-364.
20. Jin, W.; Millar, J. S.; Broedl, U.; Glick, J. M.; Rader, D. J. Inhibition of endothelial lipase causes increased HDL cholesterol levels in vivo**.** *J. Clin. Invest*. **2003**, 111, 357-362.
21. Sun, S.; Dean, R.; Jia, Q.; Zenova, A.; Zhong, J.; Grayson, C.; Xie, C.; Lindgren, A.; Samra, P.; Sojo, L.; van Heek, M.; Lin, L.; Percival, D.; Fu, J.-m.; Winther, M. D.; Zhang, Z. Discovery of XEN445: a potent and selective endothelial lipase inhibitor raises plasma HDL-cholesterol concentration in mice. Bioorg. Med. Chem. 2013, 21, 7724−7734.
22. Greco, M. N.; Connelly, M. A.; Leo, G. C.; Olson, M. W.; Powell, E.; Huang, Z.; Hawkins, M.; Smith, C.; Schalk-Hihi, C.; Darrow, A. L.; Xin, H.; Lang, W.; Damiano, B. P.; Hlasta, D. J. A thiocarbamate inhibitor of endothelial lipase raises HDL cholesterol levels in mice. Bioorg. Med. Chem. Lett. 2013, 23, 2595−2597.
23. Hangeland, J.; Abell, L. M.; Adam, L. P.; Jiang, J.; Friends, T. D.; Haque, L.; Hu, C.; Chen, A. Y.; Taylor, D. A.; Yin, X.; Harrity, T.; Basso, M.; Yang, R.; Gordon, D.; Huang, C.; Onorato, J. M.; Finlay, H.; Lawrence, M.; Wexler, R. PK/PD disconnect observed with reversible endothelial lipase inhibitor. *ACS Medicinal Chemistry Letters* (**2018**), 9(7), 673-678
24. Cuchel, M.; Raper, A. C.; Conlon, D. M.; Pryma, D. A.; Freifelder, R. H.; Poria, R.; Cromley, D.; Li, X.; Dunbar, R. L.; French, B.; Qu, L.; Farver, W.; Su, C. C.; Lund-Katz, S.; Baer, A.; Ruotolo, G.; Akerblad, P.; Ryan, C. S.; Xiao, L.; Kirchgessner, T. G.; Millar, J. S.; Billheimer, J. T.; Rader, D. J. A novel approach to measuring macrophage-specific reverse cholesterol transport in vivo in humans. *J Lipid Res.* (**2017**), 58(4), 752-762
25. Kirchgessner, Todd. G.; Sleph, P.; Ostrowski .; Lupisella, J.; Ryan, C., S..; Liu, X.; Fernando, G.; Grimm, D.; Shipkova, .; Zhang, R.; Garcia, R.; Zhu, J.; He, A.; Malone, H.; Martin, R.; Behnia, K.; Wang, Z.; Barrett, Y. C.; Garmise, R. J.; Yuan, L.; Zhang, J.; Gandhi, M. D.; Wastall, P.; Li, T.; Du, S.; Salvador, L.; Mohan R.; Cantor, G. H.; Kick, E.; Lee, J.; Frost, R. J. A. *Cell Metabolism* (**2016**), 24, 223-233
26. Johnson, J. A.; Tora, G.; Pi, Z.; Phillips, M.; Yin, X.; Yang, R.; Zhao, L.; Chen, A. Y.; Taylor, D. S,; Basso, M.; Rose, A.; Behnia, K.; Onorato, J,; Chen, X-Q.; Abell, M. L.; Lu, H.; Locke, G.; Caporuscio, C.; Galella, M.; Adam, L. P.; Gordon, D.; Wexler, R. R.; Finlay, H. J. Sulfonylated benzothiazole as inhibitors of endothelial lipase. *ACS Medicinal Chemistry Letters* (**2018**), 9(12), 1263-1268

27. Kim, S-H.; Johnson, J. A.; Jiang, J.; Parkhurst, B.; Phillips, M.; Pi, Z.; Qiao, J.; Tora, G.; Chen, A. Y.; Liu, E.; Yin, X.; Yang, R.; Zhao, L.; Taylor, D. S.; Basso, M.; Behnia, K.; Onorato, J.; Chen, X-Q.; Abell, L. M.; Lu, H.; Locke, G.; Caporuscio, C.; Adam, L. P.; Gordon, D.; Wexler, R.; Finlay, H. J. Identification of substituted benzothiazole sulfones as potent and selective inhibitors of endothelial lipase. *Bioorg. Med. Chem. Lett.* (2019), 29, 1918-1921

TOC Graphic

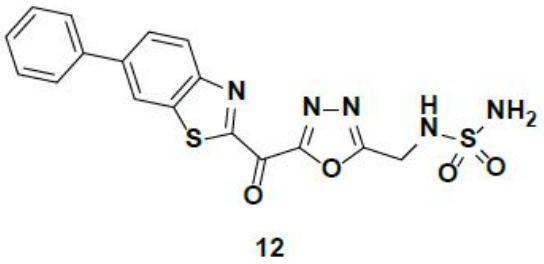

12

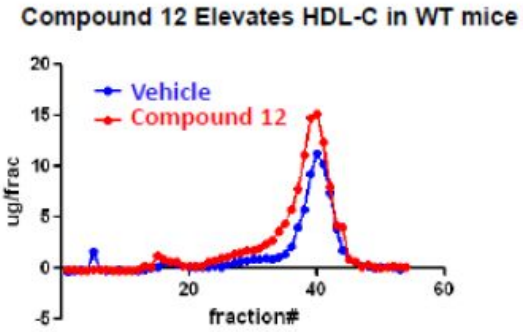
Compound 12 Elevates HDL-C in WT mice
Vehicle
Compound 12
ug/frac
fraction#
20
15
10
5
0
-5
20
40
60

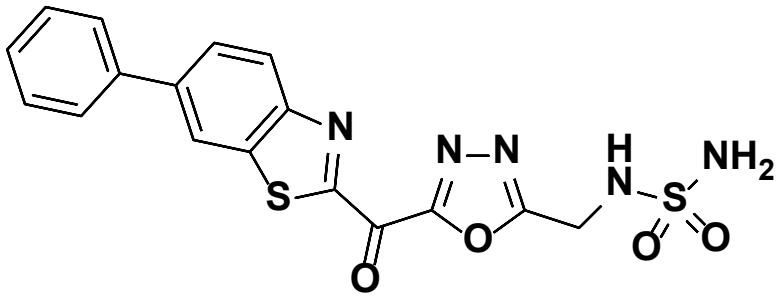
N
S
N–N
O
O
H
N
S
O
O
NH2

12

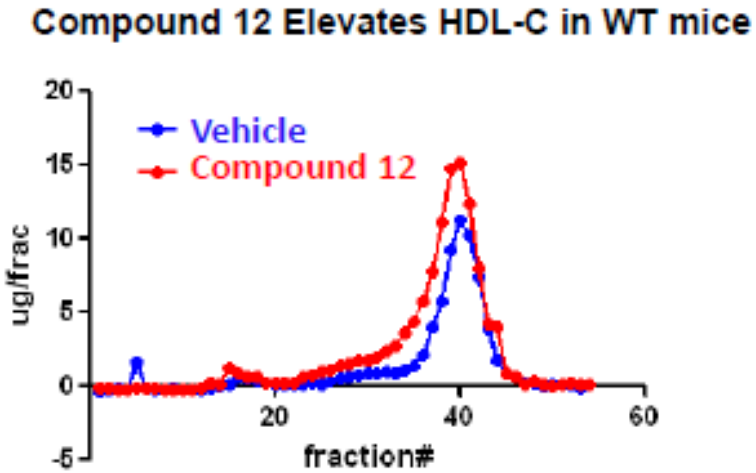
Compound 12 Elevates HDL-C in WT mice
Vehicle
Compound 12
ug/frac
20
15
10
5
0
-5
20
40
60
fraction#